SHORT-TERM CALIBRATION OF MTSAT-1R SOLAR CHANNEL USING DESERT TARGETS

Hyoung-Wook Chun, and Byung-Ju Sohn

School of Earth and Environmental Sciences, Seoul National University, Seoul, 151-747, Korea : chunhw@eosat.snu.ac.kr

In this study, we propose the calibration algorithm for the solar channel (550 ~ 900 nm) of MTSAT 1R which is the Japanese geostationary satellite launched on 26 Feb. 2005 and located at 140°E. We developed a method utilizing MODIS-derived BRDFs for the solar channel calibration over the bright desert area. Targets are selected based on the desert's brightness, spatial uniformity, temporal stability and spectral stability. The 6S model has been incorporated to account for directional effects of the surface using MODIS-derived BRDF parameters within the spectral interval in interest. Results based on the analysis for the period from November 2007 to June 2008 suggest that MTSAT-1R solar channel measurements have a low bias within 5%.

KEY WORDS: Solar channel calibration, BRDF, COMS, MTSAT-1R, MODIS, SeaWiFS

1. INTRODUCTION

The Multi-Functional Transport Satellite 1R (MTSAT 1R) succeed the Geostationary Meteorological Satellite (GMS) series as the next generation satellite series covering the East Asia and the Western Pacific regions. The Japanese Advanced Meteorological Imager (JAMI) aboard the MTSAT 1R measures the reflected solar radiation within a spectral band (550 ~ 900 nm) as well as emitted infrared radiation at 4 spectral bands. The retrieval of quantitative parameters requires absolute calibration of the radiometer and monitoring of its drift. As no in-flight calibration device is available for the solar channel, vicarious calibration is needed for producing level 1.5 data.

In this study we develop a method of utilizing satellite-derived BRDF for calculating the TOA radiance which then will be used for the solar channel calibration. Bright desert targets are chosen because the atmospheric contribution to the TOA radiance is fractionally smaller, compared to the surface contribution over the bright surface. Spatial and temporal variations of MODIS-derived nadir bidirectional reflectance distribution function (BRDF) and NDVI are examined over the Australian Simpson desert in order to select the bright surface area. Seasonally varying BRDFs over the selected targets are used as inputs to the 6S radiative transfer model to simulate visible channel radiances. And finally we estimate the calibration coefficient of MTSAT 1R and compared with the original calibration coefficient.

Corresponding author address: Byung-Ju Sohn, School of Earth and Environmental Sciences, Seoul National University, Room 501-523, e-mail : sohn@snu.ac.kr

2. METHODOLOGY

2.1 Surface characterization

Since surface reflectance varies with positions of sun and satellite, information on the bidirectional reflectance distribution function (BRDF) is necessary for accurate calculation of the TOA radiance. In this study, BRDF information derived from MODIS/TERRA measurements is used, which is from the composite of all available cloud-free, atmospherically corrected, spectral surface reflectance observations over a 16-day period with a semi-empirical, kernel-driven BRDF model (Lucht et al., 2000). The theoretical basis of this kernel-driven BRDF model is that the land surface reflectance can be modeled as a sum of three kernels representing basic scattering types: (1) isotropic scattering, (2) radiative transfer-type volumetric scattering from horizontally homogeneous leaf canopies, and (3) geometric-optical surface scattering from scenes containing 3-D objects that cast shadows and are mutually obscured from view at off-nadir angles (Lucht et al., 2000).

The black and white sky albedos are used in this study. The black sky albedo is the reflectance from direct illumination source taking places over the 2π solid angle. This albedo is derived from integration of BRDF over the hemisphere (2π solid angle), so it is a function of solar zenith angle. The black sky albedo at the solar zenith angle of 10 is used for the calculation of the spectral surface reflectance (see 2.3 section). Because the white sky albedo is the reflectance in all directions from isotropic diffuse source, it can be obtained by integrating black sky albedo over illumination hemisphere and therefore is independent of angles. The white sky albedo is used as input to the radiative transfer model, along with BRDF.

2.2 Target selection

We use the brightness, spatial uniformity, temporal stability and spectral stability as criteria for selecting bright targets (Mitchell et al. 1997). The brightness of the target is important because the impact of uncertainties on measurement and characterization leads to the relative error inversely related to the brightness. The nadir BRDF (N. BRDF) is used for the brightness test. Spatial uniformity is also important because unavoidable registration error introduces significant uncertainty into the calibration method when the surface is not spatially uniform. Cosnefroy et al. (1996) computed the coefficient of variation (CV) which was defined by the ratio of normalized standard deviation to the mean of normalized TOA reflectance on a moving 41 x 41 pixel window in the METEOSAT-4 image. In this study, CV of N. BRDF is calculated at a 5 x 5 grid (about 20 x 20 km) window. Temporal stability is considered important for the sensor drift monitoring whereas spatial homogeneity is important element for the target selection. The NDVI is used for the spectral stability check at 11 potential targets given in Fig. 1. The potential targets (marked by gray circles in Fig. 1) are chosen when N. BRDF > 0.2, CV < 0.06, temporal standard deviation < 0.06, and NDVI < 0.2.
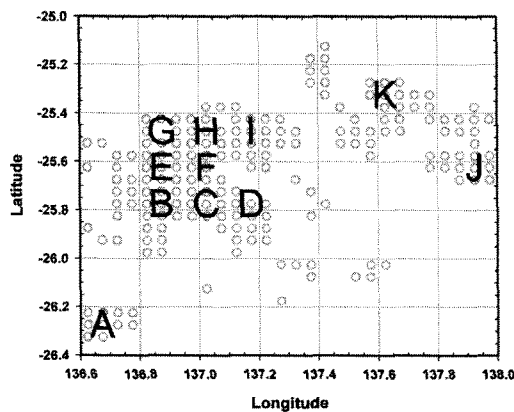

Figure 1. The location of 11 selected targets (A - K). The gray circles represent targets satisfying the target criteria.

2.3 Conversion of narrow band BRDF parameters to broad band parameters

Considering that COMS/MI solar channel will measure radiance over the broad band from 550 nm up to 800 nm, the MODIS BRDF parameters in seven bands are to be interpolated into the predefined wavelengths. The proposed method is based on the comparison of the black-sky albedo estimated at each MODIS band $\overline{\alpha}_{MO}$ (band, t arg et, time) with the surface spectra from the ASTER spectral library (http://speclib.jpl.nasa.gov). The ASTER spectral library provides the spectral black sky-albedo at a 10° solar zenith angle $\alpha_{AS}(\lambda, type)$ from 400 nm up to 14000 nm for 41 surface types. The

$\alpha_{AS}(\lambda, type)$ is converted into the spectral albedos at seven MODIS bands $\overline{\alpha}_{AS}$ (band, type) by applying MODIS response functions to $\alpha_{AS}(\lambda, type)$. Linear regression equation is obtained by relating $\overline{\alpha}_{MO}$ (band, t arg et, time) to $\overline{\alpha}_{AS}$ (band, type) . The surface type is selected at each target when the regression coefficient is largest. Then the spectral black sky albedo $\alpha(\lambda, t$ arg et, time) is estimated from $\alpha_{AS}(\lambda, type)$ by applying the regression equation of the chosen soil type. Assuming the spectral variation of black-sky albedo $\partial\alpha / \partial\lambda$ is equal to that in BRDF parameters, MODIS BRDF parameters at seven bands are interpolated to wavelength band in interest using the spectral variation of BRDF parameters.

2.4 TOA radiance simulation over desert target

The TOA radiance is simulated using the 6S radiative transfer model (Vermote et al. 1997) for the given surface and atmospheric conditions. The spectral BRDF and albedo used for the specification of surface property are derived by interpolating spectral BRDF parameters at 7 MODIS bands into ones at each 2.5 nm between from 450 to 900 nm. Because the atmospheric contribution to the TOA radiance is much weaker than the surface contribution over the bright desert, the atmospheric conditions are specified with climatological values, i.e.: total precipitable water from NCEP, total ozone from OMI, and aerosol optical thickness at 500 nm of 0.1 representing the continental aerosol model.

3. RESULT

3.1 Algorithm test using reference satellite sensor

As surface characteristics of the desert are assumed to be accurate and stable over the time, the main error sources are from the instrumental radiometric noise and uncertainties associated with inaccurate atmospheric parameters (Govaerts and Clerici, 2004). The ratios of calculated radiance to observed value over the 16-day period at each target is averaged to reduce temporal random errors. Then ratio representing the target is obtained by taking an average of pixel-based ratios in the target under the assumption that the surface characterization errors are not correlated to each other -- see Fig. 2 for the MODIS case and Fig. 3 for the SeaWiFS case.

The temporally and spatially averaged ratios for MODIS (See Fig. 2) and SeaWiFS (See Fig. 3) show that the computed radiance errors are in 5% uncertainty range except June. The ratios during June are removed using quality flag provided with BRDF parameters. The 5% uncertainty range obtained from both MODIS and SeaWiFS measurements.
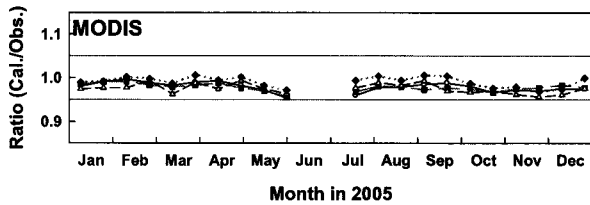
Fig. 2. The taget-averaged ratio of 6S model-calculated to the MODIS-observed value: Band 1 (open circle), band 2 (solid square), band3 (open triangle), band 4 (solid diamond). The red line represent ± 5% error.
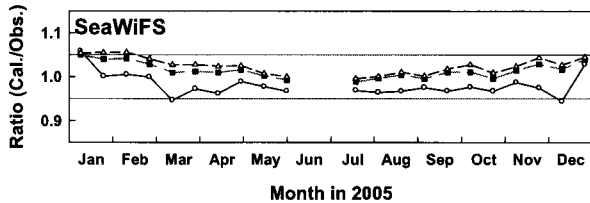

Fig. 3. Same as in Fig. 4 except for the SeaWiFS : Band 5 (open circle), band 6 (solid square), band7 (open triangle).

Table 1 shows the annual mean of spatially averaged ratio of calculated radiance to observed radiance at each MODIS and SeaWiFS bands. If we make the annual mean ratio, the relative bias between calculated and satellite-estimated values are within ±5% for all MODIS and SeaWiFS bands.

Table 1. The annual mean of spatial averaged ratio of calculated to observed radiances at each band.

Sensor	Band	Spectral range	Annual mean of Ratio
MODIS	Band 1	620 ~ 670 nm	0.971 ± 0.026
	Band 2	841 ~ 876 nm	0.970 ± 0.026
	Band 3	459 ~ 479 nm	0.975 ± 0.011
	Band 4	545 ~ 565 nm	0.988 ± 0.014
SeaWiFS	Band 5	545 ~ 565 nm	0.975 ± 0.032
	Band 6	660 ~ 680 nm	1.005 ± 0.038
	Band 7	745 ~ 785 nm	1.015 ± 0.038

3.2 MTST 1R calibration

The calibration coefficient of MTSAT 1R are retrieved using linear regression between simulated radiance and satellite observed digital count from November 2007 to June 2008. – see fig. 4. The black dashed line represents the relation between radiance and digital count using the original calibration coefficient as 0.4258. The red line represents the regression line using desert target. There are many scattered at the early March (81~88 Julian day) and late June (153~160 Julian day). These case have some problem for cloud screening.

Linear regression equation is obtained by relating observed radiance to simulated radiance for desert target every 8 day, and the time series of slope (the calibration coefficient), intercept, R^2 and RMSE are showed in Fig. 5. The slope (the calibration coefficient) is in 5% uncertainty range (gray dashed line) except for late March and early June.

4. CONCLUSION

This paper describes a solar channel calibration algorithm for the visible channel calibration using bright desert target. Surface characterization was performed over the bright Australian desert by combining the MODIS BRDF parameter with the ASTER spectral database. Simulated radiances over the selected desert targets were compared with MODIS and SeaWiFS measured spectral radiances in order to examine the feasibility of the developed calibration method. Results suggest that the relative bias between calculated and satellite-estimated radiances are within ±5% uncertainly range when a large number of pixels are averaged over all selected desert targets, suggesting that the vicarious method developed in this study is suitable for calibrating the visible senor within the suggested error range. The calibration coefficient of MTSAT 1R is retrieved within 5% error range for the original calibration coefficient (0.4258).

REFERENCES

Cosnefroy, H., M. Leroy, and X. Briottet, 1996. Selection and characterization of Saharan and Arabian desert sites for the calibration of optical satellite sensors. *Reomte Sensing Env.*, 58, pp. 101-114.

Govaerts, Y. M. and M. Clerici, 2004. Evaluation of radiative transfer simulations over bright desert calibration sites. *IEEE Trans. Geosci. Remote Sensing*, 42, pp. 176-187.

Lucht, W., C. B. Schaaf, and A. H. Strahler, 2000. An Algorithm for the Retrieval of Albedo from Space Using Semiempirical BRDF Models. *IEEE Trans. Geosci. Remote Sensing*, 38, pp. 977-998.

Mitchell, R. M., D. M. O'Brien, M. Edwards, C. C. Elsum, and R. D. Graetz, 1997. Selection and Initial characterization of bright calibration site in the Strzelecki desert, South Australia. *Canadian J. Remote Sensing*, 23, pp. 342-353.

Vermote, E. F., D. Tanre, J. L. Deuze, M. Herman, and J. J. Morcrette, 1997. Second simulation of the satellite signal in the solar spectrum, 6S: An overview. *IEEE Trans. Geosci. Remote Sensing*, 35, pp. 675-686.
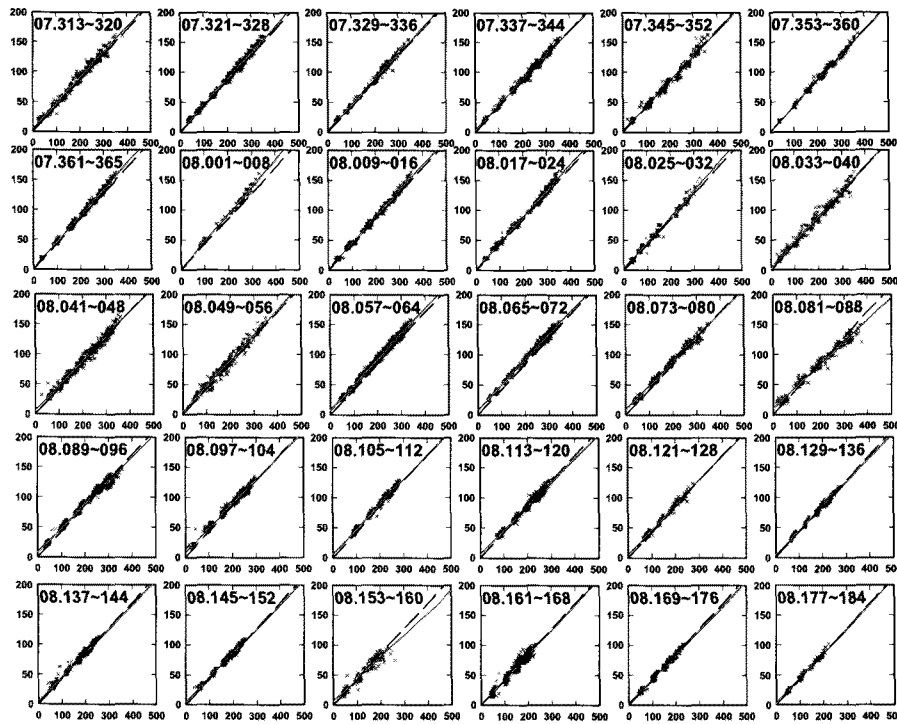
Fig. 4. The scatter plot of simulated TOA radiance at MTSAT 1R visible band and observed digital count.
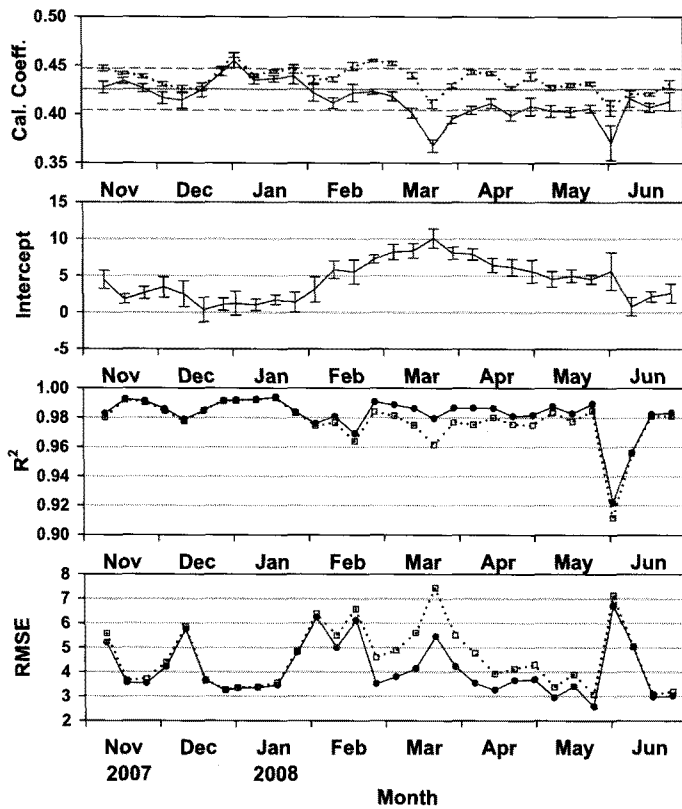

Fig. 5. Time series of calibration coefficient (slope), intercept, R^2, and RMSE for MTSAT 1R visible band using desert target. The red solid line represent statistics values for normal linear regression, and the blue dotted line for linear regression though the origin.